

# Extended Neutral Gas Around $z \sim 0.5$ Galaxies: Properties of Damped Ly $\alpha$ Absorbing Galaxies

Hsiao-Wen Chen

*Center for Space Research, Massachusetts Institute of Technology,  
Cambridge, MA 02139, U.S.A.*

## Abstract.

I review current results from searching for galaxies giving rise to damped Ly $\alpha$  absorbers (DLAs) at  $z < 1$ . Using 14 confirmed DLA galaxies, I further show that intermediate-redshift galaxies possess large HI envelope out to  $24-30 h^{-1}$  kpc radius. The photometric and spectral properties of these galaxies confirm that DLA galaxies are drawn from the typical field population, and not from a separate population of low surface brightness or dwarf galaxies. Comparisons of the ISM abundances of the DLA galaxies and the metallicities of the absorbers at large galactic radii suggest that some DLAs originate in the relatively unevolved outskirts of galactic disks.

## 1. Background

Damped Ly $\alpha$  absorbers (DLAs) observed in the spectra of background QSOs probe neutral gas regions commonly seen in nearby galaxies (with HI column density  $N(\text{HI}) \geq 2 \times 10^{20} \text{ cm}^{-2}$ ). In principle, these DLAs offer a means of studying the galaxy population at high redshift using galaxies selected uniformly based on known neutral gas content, rather than optical brightness or color. Optical spectroscopic surveys for DLAs have demonstrated that DLAs dominate the mass density of neutral gas in the universe and that they contain roughly enough gas at  $z = 3.5$  to form the bulk of the stars in present-day galaxies (Wolfe et al. 1995; Storrie-Lombardi & Wolfe 2000; Péroux et al. 2002; Prochaska & Herbert-Fort 2004). But chemical abundance analyses of DLAs at redshift  $z < 1.6$  yield sub-solar metallicities in the neutral gaseous clouds (Pettini et al. 1999; Prochaska et al. 2003), suggesting that they do not trace the bulk of star formation and are likely to represent a biased sample of galaxies. Because metallicity varies as functions of morphological type and galactocentric distance, it is impossible to understand the origin of DLAs without first identifying the absorbing galaxies.

Identifying the optical counterpart of the DLAs has been a challenging task, because these galaxies are faint and located at small projected distances to the background, bright QSOs (as implied by the intrinsic high column density of the absorbers). Le Brun et al. (1997) reported candidate absorbing galaxies toward seven QSO lines of sight with known DLAs based on high spatial resolution HST/WFPC2 images. These galaxies exhibit a wide range in morphological types, from luminous spiral galaxies, to compact objects, and to low surface brightness galaxies. In two fields, they also identify possible groups of galaxies that are associated with the DLAs. In contrast, Rao et al. (2003) collected

Table 1. Summary of Confirmed DLA Galaxies at  $z < 1$ 

QSO (1)	$z_{\text{QSO}}$ (2)	$z_{\text{DLA}}$ (3)	$\log N(\text{H I})$ (4)	$\Delta\theta$ ( $''$ ) (5)	$\rho \times h^a$ (kpc) (6)	$AB$ (7)	$M_{AB}(B)^b$ $-5 \log h$ (8)	Morphology (9)
TON 1480 .....	0.614	0.0036	20.34	114.0	5.94	$B = 11.5$	-18.7	S0
HS1543+5921 .....	0.807	0.009	20.35	2.4	0.31	$R = 16.5$	-15.3	LSB
PKS0439-433 ..	0.593	0.101	19.85	3.9	5.13	$I = 17.2$	-19.6	disk
Q0738+313 .....	0.635	0.2212	20.90	5.7	14.23	$I = 20.9$	-17.7	compact
Q0809+483 .....	0.871	0.4368	20.80	1.5	5.9	$R = 19.9$	-20.3	disk
B20827+243 .....	0.939	0.525	20.30	5.8	25.42	$R = 21.0$	-20.0	disk
PKS1629+120 .....	1.795	0.532	20.70	3.0	13.24	$R = 21.6$	-19.2	disk
LBQS0058+0155 ..	1.954	0.613	20.08	1.2	5.67	$R = 23.7$	-17.6	disk
HE1122-1649 .....	2.400	0.681	20.45	3.6	17.66	$I = 22.4$	-18.8	compact
FBQS 0051+0041 ..	1.190	0.740	20.40	3.3	16.87	$I = 22.4$	-18.6	compact
EX0302-2223 .....	1.400	1.001	20.36	3.3	18.65	$R = 23.2$	-19.3	Irr
PKS 1127-145 ..	1.187	0.313	21.71	3.8	12.2	$R = 22.4$	-16.8	Irr
				3.8	12.2	22.1	-17.4	compact
				9.8	31.5	19.1	-20.1	disk
				17.5	56.2	18.9	-20.3	disk
AO0235+164 .....	0.940	0.524	21.70	2.1	9.4	$I = 20.2$	-20.3	compact
				6.4	28.0	$I = 20.9$	-19.7	compact
FBQS 1137+3907 ..	1.020	0.719	21.10	2.5	12.6	$K = 21.4$	-18.8	compact
				1.5	7.6	$K = 21.7$	-18.5	Irr

a. A  $\Lambda$  cosmology,  $\Omega_M = 0.3$  and  $\Omega_\Lambda = 0.7$  with  $h = H_0/(100 \text{ km s}^{-1} \text{ Mpc}^{-1})$  is adopted throughout.b.  $M_{AB*}(B) - 5 \log h = -19.6$  (Ellis et al. 1996).Table 2. Summary of Candidate DLA Galaxies at  $z < 1$ 

QSO (1)	$z_{\text{QSO}}$ (2)	$z_{\text{DLA}}$ (3)	$\log N(\text{H I})$ (4)	$\Delta\theta$ ( $''$ ) (5)	$\rho \times h$ (kpc) (6)	$AB$ (7)	$M_{AB}(B)$ $-5 \log h$ (8)	References (9)
Q0738+313 .....	0.635	0.0912	21.18	...	...	$K > 17.8$	> -18.8	1,2
PKS0952+179 .....	1.472	0.2390	21.32	...	...	...	...	3
PKS1229-021 .....	1.038	0.3950	20.60	1.4	$\approx 5.2$	$R = 22.1$	$\approx -18.4$	4
Q1209+107 .....	2.191	0.6295	20.48	1.6	$\approx 7.7$	$R = 21.6$	$\approx -20.5$	5
PKS1622+23 .....	0.927	0.6563	20.36	...	...	$R > 24.5$	> -16.9	6
Q1328+307 .....	0.849	0.692	21.30	2.0	$\approx 10$	$I = 22.1$	$\approx -19.3$	5
PKS0454+039 .....	1.345	0.8596	20.76	0.8	$\approx 4.3$	$R = 24.2$	$\approx -19.0$	4,5

1. Turnshek et al. (2001); 2. Cohen (2001); 3. Rao et al. (2003); 4. Steidel et al. (1994); 5. Le Brun et al. (1997);  
6. Steidel et al. (1997).

a sample of 14 candidate or confirmed DLA galaxies, and argued that low-luminosity dwarf galaxies dominate the DLA galaxy population with  $\approx 50\%$  of the DLAs originating in galaxies of luminosity  $L \leq 0.25 L_*$ .

Despite extensive searches in the past decade, the number of confirmed DLA galaxies remains relatively small. Of all the 23 DLA systems known at  $z \leq 1$ , 14 have been identified with their host galaxies using either spectroscopic or photometric redshift techniques (see section 2 for a complete list). Here I will first review current results from searching for  $z < 1$  DLA galaxies. Then I will compare the optical properties of the absorbing galaxies, such as  $B$ -band luminosity, stellar content, and rotation velocity, with known properties of the absorbers, such as  $N(\text{H I})$  and metallicity.

## 2. A Sample of DLA Galaxies at $z < 1$

A list of 14 DLA galaxies confirmed using either spectroscopic or photometric redshift techniques is presented in Table 1 (see also Chen & Lanzetta 2003 for a list of references and Lacy et al. 2003 for new additions). It is interesting to note that the three highest- $N(\text{H I})$  DLAs are found to be associated with a group of galaxies within a small projected distance (the last three DLAs in Table 1). In addition, the DLAs toward TON 1480 and HS1543+5921 were

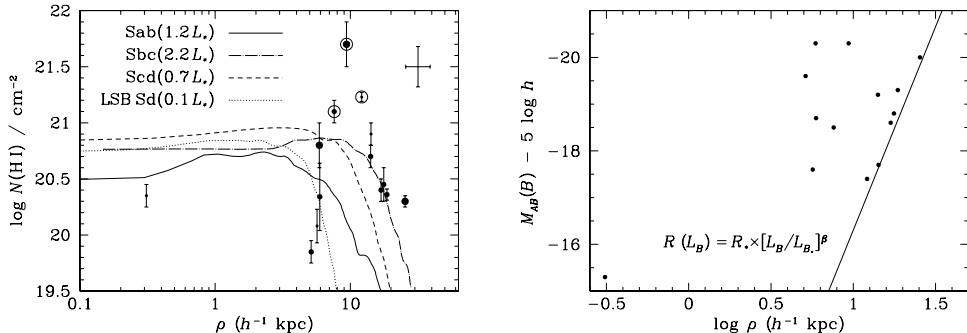


Figure 1. Left:  $N(\text{HI})$  distribution versus galaxy impact parameter  $\rho$  from 14 DLA galaxies (points), compared to the mean HI profiles of nearby galaxies of different morphological type and intrinsic luminosity shown in curves. Right: The distribution of  $B$ -band absolute magnitude versus  $\rho$  for the 14 galaxies. The solid line shows the best-fit scaling relation that describes the apparent envelope stretching to larger  $\rho$  at brighter  $M_{AB}(B)$ .

discovered in targeted searches of DLAs, with a prior knowledge of the presence of a foreground galaxy within a small radius from the sightline, while the rest of the absorbers were identified in a survey of random QSO sightlines.

Additional efforts were made to search for the absorbing galaxies of seven DLAs listed in Table 2. Candidate galaxies were found for the DLAs toward PKS0952+179, PKS1229–021, Q1209+107, Q1328+307, and PKS0454+039 based on their close proximity to the QSO sightlines, while no candidates were found for the DLAs toward Q0738+313 and PKS1622+23 after extensive surveys.

The collection of 14 confirmed DLA galaxies represents the first large DLA-selected galaxy sample, which allows us (1) to determine the neutral gas cross-section of intermediate-redshift galaxies; (2) to establish an empirical correlation between the kinematics and metallicity of the absorbers and those of the absorbing galaxies; and (3) to study the disk population at intermediate redshift using galaxies selected uniformly based on known neutral gas content, rather than optical brightness or color.

### 3. HI Extent of Intermediate-redshift Galaxies

Figure 1 shows  $N(\text{HI})$  versus  $\rho$  for the 14 galaxy and DLA pairs in the left panel. Mean HI surface density profiles measured from 21-cm observations of nearby galaxies of different morphological type and intrinsic luminosity are presented in different curves (the mean HI profiles for Sab, Sbc, and Scd galaxies were digitized from Cayatte et al. 1994; the curve for LSB Sd was provided by Uson & Matthews 2003). The scatter of  $N(\text{HI})$  at the Holmberg radii and the scatter of the neutral gaseous extent at  $N(\text{HI}) = 10^{20} \text{ cm}^{-2}$  from 21-cm data for Sd-type galaxies are marked by the error bar in the upper-right corner (Cayatte et al. 1994). The three DLAs found in groups of galaxies are marked in circles. The size of the points indicates the intrinsic brightness of the galaxies:  $M_{AB}(B) - 5 \log h \leq -19.6$  (large),  $-19.6 < M_{AB}(B) - 5 \log h \leq -18$  (medium),

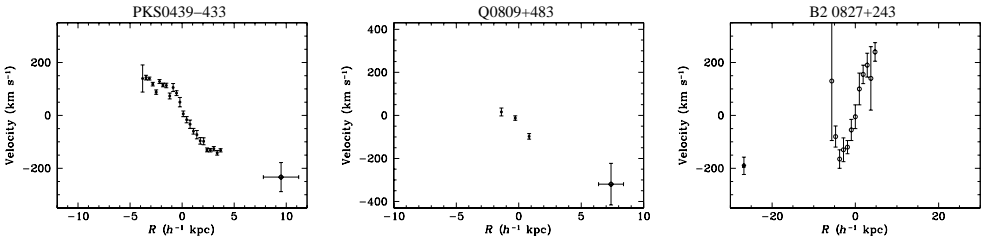


Figure 2. Rotation velocity measurements of three DLA galaxies versus galactocentric radius  $R$  along the disk, in comparison to the velocity difference between the galaxies and the DLA deprojected to the optical disks at large  $R$ . The velocity measurements presented in the plot has been corrected for the inclination of the optical disk. Measurements for the galaxy toward Q0827+243 were digitized from Steidel et al. (2002).

and  $M_{AB}(B) - 5 \log h > -18$  (small). Despite the apparent large scatter in the  $N(\text{HI})$  distribution, we see two interesting features. First, the  $N(\text{HI})$  in DLAs is not grossly different from the mean HI distribution of nearby galaxies, although we note that measurements obtained in 21-cm observations are smoothed over a finite beam size. Second, while the HI extent of these intermediate-redshift galaxies appears to be comparable to that of nearby galaxies, most DLAs tend to lie at slightly larger radii of the absorbing galaxies for a given  $N(\text{HI})$ .

The extent of neutral gas around intermediate-redshift galaxies may be quantified based on the distribution of  $M_{AB}(B)$  versus  $\rho$  of known galaxy-DLA pairs. The right panel of Figure 1 presents the  $M_{AB}(B)$  versus  $\rho$  distribution for 14 galaxy-DLA pairs. It shows that the data points are enclosed in an envelope that stretches to larger  $\rho$  at brighter  $M_{AB}(B)$ , indicating a finite size of the underlying HI disks. Chen & Lanzetta (2003) adopted a power-law model to characterize this envelope

$$\frac{R}{R_*} = \left( \frac{L_B}{L_{B_*}} \right)^\beta \quad (1)$$

and found  $R_* = 24 - 30 h^{-1}$  kpc and  $\beta = 0.26 - 0.29$  for  $M_{AB_*}(B) - 5 \log h = -19.6$  (Ellis et al. 1996).

In addition, rotation curve measurements along the major axis of the optical disk of the galaxies toward PKS0439-433 ( $z_{\text{DLA}} = 0.101$ ), Q0809+483 ( $z_{\text{DLA}} = 0.437$ ), and B2 0827+243 ( $z_{\text{DLA}} = 0.525$ ) are presented in Figure 2. Note that the observed inner slope of these rotation curves is expected to be shallower than the intrinsic shape because of a “beam-smearing” effect caused by seeings that has not been removed from the data. Nevertheless, the observations allow us to compare the relative motions between the ionized gas in the inner ISM and the neutral gaseous clouds at large galactocentric distances, and to obtain a robust measurement of the rotation speed of galaxy disks at intermediate redshifts. In all three cases, we observe consistent rotation motion between the optical disks and the neutral gaseous clouds. These results confirm that galaxies with disk-like stellar morphologies at intermediate redshifts possess large rotating HI disk out to  $24 - 30 h^{-1}$  kpc, a factor of  $\approx \sqrt{2}$  larger than what is observed in local disk galaxies (Rosenberg & Schneider 2002).

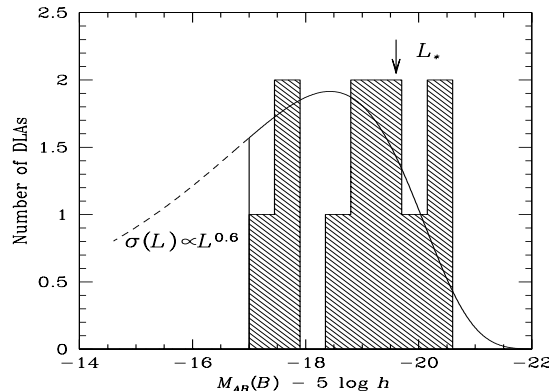


Figure 3. Luminosity distribution of DLA galaxies (the shaded histogram), in comparison to predictions (the solid curve) from adopting a Schechter luminosity function, which is characterized by  $M_{AB*}(B) = -19.6$  and  $\alpha = -1.4$ , and the best-fit scaling relation. The model has been normalized to match the total number of DLA galaxies observed in the homogeneous sample. The dashed curve indicates the expected number of DLAs produced by these fainter galaxies if their neutral gas cross section were to be characterized by the same scaling relation of the more luminous ones.

#### 4. Photometric Properties of the DLA Galaxies

A comparison of the luminosity distribution of the DLA galaxies and models derived from adopting the scaling relation of equation (1) and a known galaxy luminosity function allows us to determine how the neutral gas cross section is distributed among galaxies of different intrinsic luminosity. The results are presented in Figure 3 for 12 confirmed DLA galaxies selected from random lines of sight (excluding the two systems toward TON 1480 and HS1543+5921; see § 2). Figure 3 shows that the observed luminosity distribution of the DLA galaxies agrees well with what is expected from the field galaxy population, if all field galaxies possess an extended HI envelope described by equation (1). In addition, it shows that  $\approx 30\%$  of the DLAs originate in dwarf galaxies of  $L_B \leq 0.25 L_{B*}$ ,  $\approx 50\%$  of the DLAs originate in sub- $L_*$  galaxies of  $0.25 L_{B*} \leq L_B \leq L_{B*}$ , and  $\approx 20\%$  of the DLAs originate in super- $L_*$  galaxies of  $L_B \geq L_{B*}$ . Including candidate DLA galaxies listed in Table 2 does not alter the luminosity distribution.

High spatial resolution images of low-redshift DLA galaxies available in the literature already display a wide range of morphological types among galaxies that are associated with DLAs (Le Brun et al. 1997; Turnshek et al. 2001; Chen & Lanzetta 2003). Figure 4 presents individual images of five additional DLAs for which moderate resolution spectra of the absorbing galaxies are available (see § 5). The summary in Table 1 indicates that of all the 14 confirmed DLA galaxies, 43% are disk dominated, 22% are bulge dominated, 14% are irregular, and 21% are in galaxy groups, confirming that DLAs originate in galaxies of different morphologies and are associated with a variety of galaxy environments.

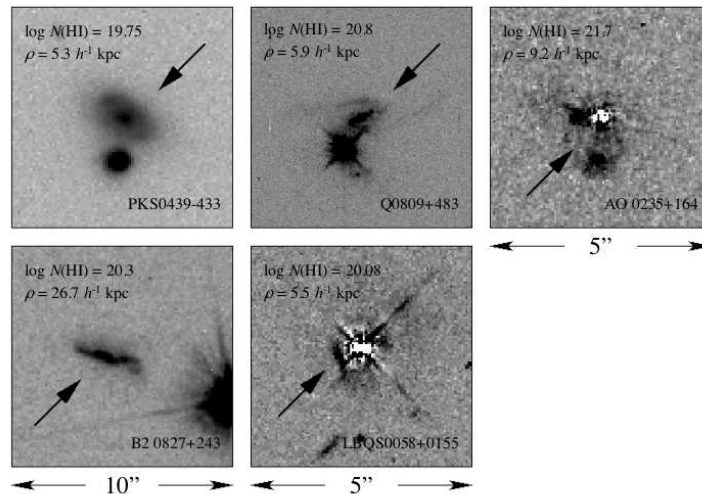


Figure 4. Direct images of five DLA galaxies at  $z < 0.65$ , showing a range of morphologies. The images are 10 arcsec on a side for the fields toward PKS0439–433 and B2 0827+243 and 5 arcsec for the rest. Field orientation is arbitrary. The light from the background QSOs toward AO 0235+164 and LBQS0058+0155 have been subtracted to bring out the faint features of the absorbing galaxies (Chen et al. 2004).

## 5. Spectral Properties of the DLA Galaxies

Figure 5 shows optical spectra of six DLA galaxies, four of which (toward PKS0439–433, Q0738+313, AO 0235+164, and B2 0827+243) are previously known, and two (toward Q0809+483 and LBQS0058+0155) are confirmed in a recent spectroscopic study (Chen, Kennicutt, & Rauch 2004). The spectra exhibit a range of properties in the ISM, from post-starburst, to normal disks, and to starburst systems, again supporting the notion that DLA galaxies are drawn from the typical field population.

Strong-line oxygen abundances for three DLA galaxies based on the  $R_{23}$  calibrator are shown in Figure 6 at galactocentric radius  $R \sim 0$ . Although the  $R_{23}$  index may systematically overestimate the oxygen abundance by 0.2–0.5 dex (Kennicutt et al. 2003), the photometric and spectral properties of these DLA galaxies are consistent with the luminosity and  $R_{23}$ -based metallicity relation of field galaxies (Kobulnicky & Zaritsky 1999). Comparisons with the metallicities of the DLAs at large  $R$  suggest that these three DLA systems originate in the relatively unevolved outskirts of galactic disks. This in turn supports the scenario in which the low metal abundances observed in DLA systems result from a gas cross-section selection bias, which favors large impact parameters.

**Acknowledgments.** I would like to thank Rob Kennicutt and Michael Rauch for allowing me to discuss some of the results in advance of publication. This research was supported in part by NASA through a Hubble Fellowship grant HF-01147.01A from the Space Telescope Science Institute, which is operated by the Association of Universities for Research in Astronomy, Incorporated, under NASA contract NAS5-26555.

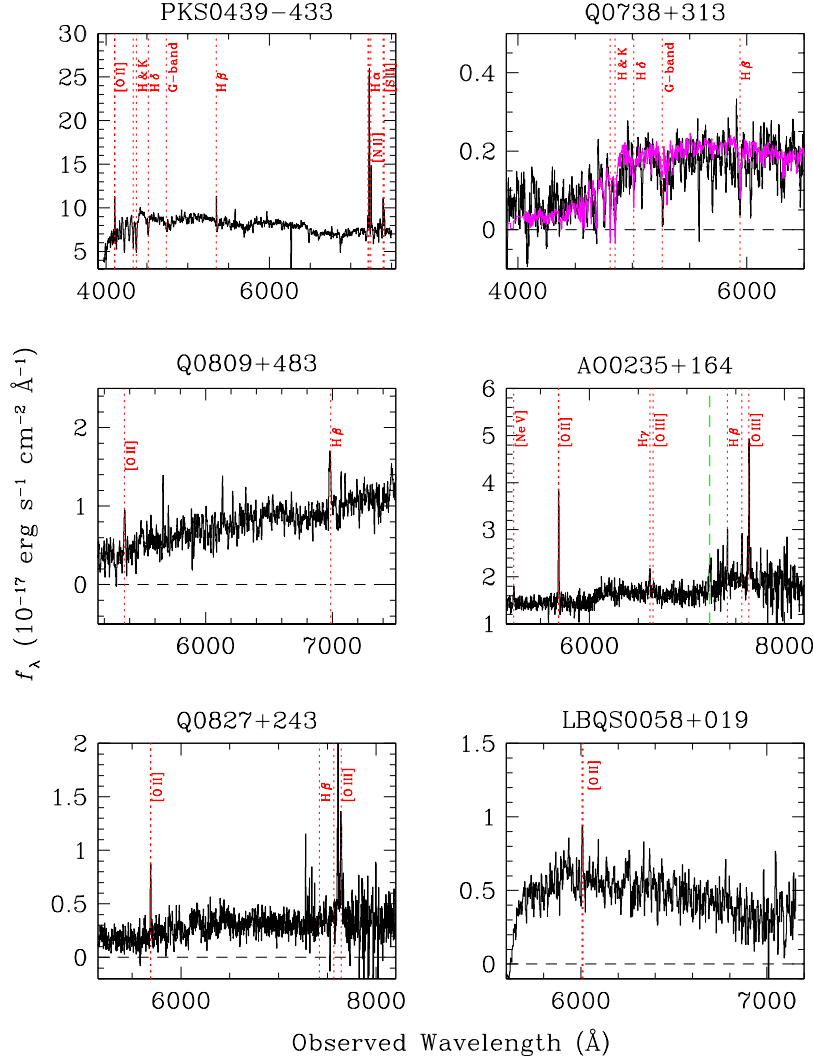


Figure 5. Moderate-resolution spectra of six DLA galaxies toward PKS0439-433 ( $z_{\text{DLA}} = 0.101$ ), Q0738+313 ( $z_{\text{DLA}} = 0.2212$ ), Q0809+483 ( $z_{\text{DLA}} = 0.437$ ), AO 0235+164 ( $z_{\text{DLA}} = 0.524$ ), B2 0827+243 ( $z_{\text{DLA}} = 0.525$ ), and LBQS0058+019 ( $z_{\text{DLA}} = 0.525$ ). Strong emission-line features of the galaxies are marked with red dotted lines. Contaminating [O II] emission feature from the background QSO AO0235+164 ( $z_{\text{QSO}} = 0.94$ ) is marked with green dashed line. All but two galaxies show spectral features of a typical disk galaxy. The spectrum of the DLA galaxy toward Q0738+313 exhibits a pronounced 4000-Å flux discontinuity and a strong Ca II doublet, in good agreement with a 2.6-Gyr old post-starburst model spectrum (the thin magenta curve) generated by the Bruzual & Charlot stellar population synthesis code (2003). The DLA galaxy toward AO 0235+164 displays mixed spectral features of both an active nucleus and starburst system, as expected from the complex morphology shown in Figure 4.

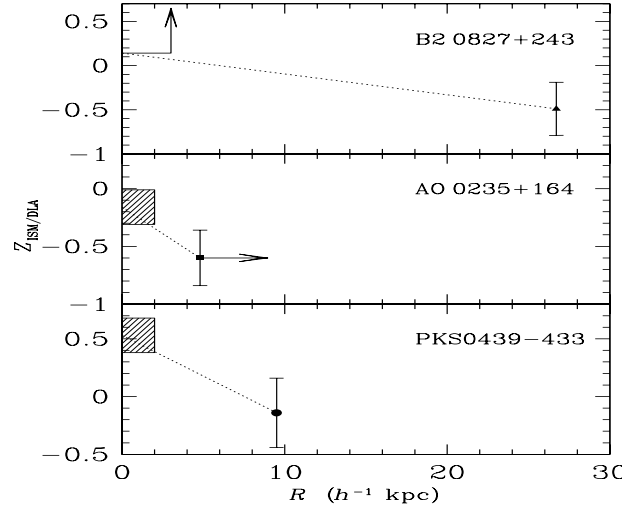


Figure 6. Abundance decrement observed from the inner ISM of the absorbing galaxies to the neutral gas at large galactocentric radii for three DLA systems. Shaded box indicate the mean oxygen abundance averaged over the inner stellar disk, including uncertainties. The  $R_{23}$  calibrator may systematically overestimate the oxygen abundance by 0.2–0.5 dex, reducing the decrement accordingly. Metallicities of the absorbers are estimated based on the observed Fe abundance, corrected for dust depletion (Chen et al. 2004). All abundance measurements are normalized to their respective solar values according to  $Z \equiv \log(X/H) - \log(X/H)_{\odot}$ .

## References

Bruzual, G. & Charlot, S. 2003, MNRAS, 344, 1000  
 Cayatte, V., Kotanyi, C., Balkowski, C., & van Gorkom, J.H. 1994, AJ, 107, 1003  
 Chen, H.-W. & Lanzetta, K. M. 2003, ApJ, 597, 706  
 Chen, H.-W., Kennicutt, R. C. Jr., & Rauch, M. 2004, ApJ submitted  
 Cohen, J.G. 2001, AJ, 121, 1275  
 Ellis, R.S. et al. 1996, MNRAS, 280, 235  
 Kennicutt, R.C. Jr., Bresolin, F., & Garnett, D.R. 2003, ApJ, 591, 801  
 Kobulnicky, H. A. & Zaritsky, D. 1999, ApJ, 511, 118  
 Le Brun, F., Bergeron, J., Boissé, P., & Deharveng, J.M. 1997, A&A, 321, 733  
 Péroux, C. et al. 2002, Ap&SS, 281, 543  
 Pettini, M., Ellison, S.L., Steidel, C.C., & Bowen, D.V. 1999, ApJ, 510, 576  
 Prochaska, J. X. et al. 2003, ApJS, 147, 227  
 Prochaska, J. X. & Herbert-Fort, S. 2004, PASP, 116, 622  
 Rao, S.M. et al. 2003, ApJ, 595, 94  
 Rosenberg, J.L. & Schneider, S.E. 2003, ApJ, 585, 256  
 Steidel, C.C., Pettini, M., Dickinson, M., & Persson, S.E. 1994, AJ, 108, 2046  
 Steidel, C.C. et al. 1997, ApJ, 480, 568  
 Steidel, C.C. et al. 2002, ApJ, 570, 526  
 Storrie-Lombardi, L.J. & Wolfe, A.M. 2000, ApJ, 543, 552  
 Turnshek, D.A. et al. 2001, ApJ, 553, 288  
 Uson, J. M., & Matthews, L. D. 2003, AJ, 125, 2455  
 Wolfe, A.M., Lanzetta, K.M., Foltz, C.B., & Chaffee, F.H. 1995, ApJ, 454, 698